

# FREQUENCY-DOMAIN ADAPTIVE MULTIDELAY ALGORITHM WITH SPARSENESS CONTROL FOR ACOUSTIC ECHO CANCELLATION

Pradeep Loganathan<sup>1</sup>, Xiang (Shawn) Lin<sup>1</sup>, Andy W.H. Khong<sup>2</sup>, Patrick A. Naylor<sup>1</sup>

<sup>1</sup> Electrical and Electronic Engineering,  
Imperial College, London, United Kingdom  
email: {pradeep.loganathan, shawn.lin, p.naylor}@ic.ac.uk

<sup>2</sup> Electrical and Electronic Engineering,  
Nanyang Technological University, Singapore  
email: andykhong@ntu.edu.sg

## ABSTRACT

A frequency-domain adaptive algorithm for acoustic echo cancellation is proposed. This new algorithm dynamically adjusts its step-size according to the sparseness variation in acoustic impulse responses that arise in a mobile environment. Inheriting the beneficial properties of both the fast convergence of the improved proportionate normalized least mean squares (IPNLMS) and the efficient implementation of the multidelay filtering (MDF) algorithm, the proposed sparseness-controlled improved proportionate MDF (SC-IPMDF) algorithm is evaluated using white Gaussian noise (WGN) and speech input signals with acoustic impulse responses of various degrees of sparseness. Simulation results show an improved performance over the MDF and improved proportionate MDF (IPMDF) algorithms with only a modest increase in computational complexity.

## 1. INTRODUCTION

With recent developments of hands-free mobile telephony, acoustic echo due to the coupling between the loudspeaker and microphone has been found to significantly degrade user experience in terms of perceived voice quality in a variety of applications such as in-vehicle communications and teleconferencing [1]. A typical acoustic echo cancellation (AEC) set up for a Loudspeaker-Room-Microphone system (LRMS) is shown in Fig. 1. Defining the tap-input vector  $\mathbf{x}(n) = [x(n) \dots x(n-L+1)]^T$  and the  $L$ -tap unknown acoustic impulse response (AIR)  $\mathbf{h}(n) = [h_0(n) \dots h_{L-1}(n)]^T$  with  $[\cdot]^T$  being the vector transposition, the LRMS output signal can be given by

$$y(n) = \mathbf{h}^T(n)\mathbf{x}(n) + w(n), \quad (1)$$

where  $w(n)$  is additive noise. The objective of AEC is hence to avoid  $y(n)$  from being transmitted back to the far-end loudspeaker. This can be achieved by employing adaptive algorithms such as the normalized least-mean-square (NLMS) algorithm [2], where  $\mathbf{h}(n)$  is modeled by an adaptive filter  $\hat{\mathbf{h}}(n) = [\hat{h}_0(n) \dots \hat{h}_{L-1}(n)]^T$  which minimizes the *a priori* error function

$$e(n) = y(n) - \hat{\mathbf{h}}^T(n-1)\mathbf{x}(n). \quad (2)$$

The tracking capabilities of these NLMS-based algorithms can also be exploited to cope with the time-varying nature of AIRs which is due to, for example, movement of the acoustic source or changes in the acoustic environment.

Recently, it has been realized that AIRs such as occur in AEC are to some extent sparse by an amount which is also time-varying [3]. It was shown in [4] that shorter distance between the loudspeaker and microphone gives rise to a more

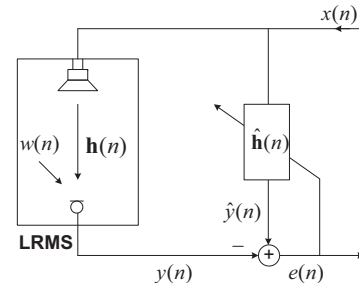


Figure 1: Adaptive system for acoustic echo cancellation (AEC) in a Loudspeaker-Room-Microphone system (LRMS).

sparse AIR. For hands-free teleconferencing where wireless microphones attached to moving users are used along with a fixed loudspeaker, the time variation of sparseness can be significant. Additionally, in outdoor and urban environments where reflections of the speech signals are considerably reduced, the sparseness of the AIR can be much greater than typical indoor environments and equally, if not more, variable. Therefore, adaptive AEC algorithms robust to sparse-ness variation of the AIRs are highly desirable.

One of the first algorithms proposed to exploit the sparse-ness of the impulse response in the context of network echo cancellation (NEC) [1] is the proportionate NLMS (PNLMS) algorithm [5]. The network impulse response is typically of length 64-128 ms and characterized by an unknown bulk delay dependent on network loading, encoding and jitter buffer delays [6]. Such response comprises an “active” region for only 8-12 ms and a dominating “inactive” region where coefficients magnitudes are close to zero, causing the impulse response sparse. The PNLMS algorithm employs a step-size for each coefficient of the adaptive filter that is proportionate to its magnitude at each iteration. However, PNLMS is well known to suffer from slow convergence when estimating dispersive AIRs [7]. The improved PNLMS (IPNLMS) algorithm [8] addresses this problem by incorporating both proportionate and NLMS adaptation at the cost of requiring twice as many multiplications per iteration as NLMS.

Frequency-domain adaptive algorithms such as the fast-LMS (FLMS) algorithm [9] have become popular because of their efficient implementation. One of the drawbacks, however, is the delay introduced between the input and output, which is equivalent to the length of the adaptive filter  $L$ . For AIRs with several hundreds of coefficients, this delay can be significant. To overcome this, the multidelay filtering (MDF) algorithm was proposed in [10] to partition the adaptive filter

into blocks each of length  $N$  such that the delay is reduced by a factor of  $K = L/N$ , although  $K = 1$  is the optimum choice in terms of computational complexity. Combining proportionate updating of filter coefficients, the improved proportionate MDF (IPMDF) algorithm [11] achieves a fast convergence with a low delay for  $K > 1$  in NEC, and a similar improvement has also been shown in [12] for blind estimation of multichannel AIRs.

The literature of adaptive sparse system identification seems rich, but the time variation of sparseness is rarely addressed. In [13], a sparseness-controlled IPNLMS (SC-IPNLMS) algorithm for NEC was proposed, where the sparseness of  $\hat{\mathbf{h}}(n)$  at each iteration is computed and utilized to determine the step-size at the next iteration. More recently, the SC-PNLMS algorithm [4] also achieves fast convergence by dynamically adjusting step-size according to time-varying sparseness of AIRs in the context of AEC.

In this paper, we propose to integrate sparseness control into the MDF domain and develop a *low-delay* and *fast tracking* frequency-domain adaptive algorithm for AEC. The classic IPNLMS, MDF and IPMDF algorithms are first reviewed in Section 2. We then show, in Section 3, how the sparseness variation of the adaptive filter can be exploited to determine the proportionate step-size at each iteration. Incorporating such sparseness variation with the MDF structure, the proposed sparseness-controlled IPMDF (SC-IPMDF) algorithm is developed. Simulation results shown in Section 5 demonstrate a faster tracking performance for both sparse and dispersive AIRs compared to MDF and IPMDF algorithms in the context of AEC.

## 2. ALGORITHMS REVIEW

### 2.1 The IPNLMS algorithm

The IPNLMS algorithm [8] was proposed based on the well-known NLMS algorithm [2]. NLMS-based adaptive algorithms can generally be described by (2) and the following set of equations:

$$\hat{\mathbf{h}}(n) = \hat{\mathbf{h}}(n-1) + \frac{\mu \mathbf{Q}(n-1) \mathbf{x}(n) e(n)}{\mathbf{x}^T(n) \mathbf{Q}(n-1) \mathbf{x}(n) + \delta}, \quad (3)$$

$$\mathbf{Q}(n-1) = \text{diag}\{q_0(n-1) \dots q_{L-1}(n-1)\}, \quad (4)$$

where  $\mu$  is the step-size and  $\delta$  is the regularization parameter. The  $L \times L$  diagonal matrix  $\mathbf{Q}(n)$  is introduced to control the step-size for each filter coefficient. Since a uniform  $\mu$  is employed for all filter coefficients in NLMS,  $\mathbf{Q}(n) = \mathbf{I}_{L \times L}$  with  $\mathbf{I}_{L \times L}$  being an  $L \times L$  identity matrix. The PNLMS algorithm [5] assigns higher step-sizes for coefficients with higher magnitude using the control matrix  $\mathbf{Q}(n)$ . To improve the convergence speed of NLMS on sparse impulse response and for PNLMS on dispersive impulse response, the IPNLMS algorithm was proposed to combine proportionate (PNLMS) and non-proportionate (NLMS) adaptation using a weighting factor  $\alpha_{\text{IP}}$  such that the diagonal elements of  $\mathbf{Q}(n)$  are given by

$$q_l(n) = \frac{1 - \alpha_{\text{IP}}}{2L} + \frac{(1 + \alpha_{\text{IP}})|\hat{h}_l(n)|}{2\|\hat{\mathbf{h}}(n)\|_1 + \varepsilon}, \quad 0 \leq l \leq L-1, \quad (5)$$

where  $\|\cdot\|$  represents the absolute value,  $\|\cdot\|_1$  denotes the  $l_1$ -norm and  $\varepsilon$  is a small constant.

In order to achieve the same steady-state performance as that of NLMS given the same step-size, the regularization parameter in (3) for IPNLMS should be taken as  $\delta_{\text{IP}} = (1 - \alpha_{\text{IP}})/(2L)\delta_{\text{NLMS}}$  [8]. As can be seen from (5), IPNLMS is equivalent to NLMS for  $\alpha_{\text{IP}} = -1$ , and PNLMS for  $\alpha_{\text{IP}} = 1$ . In other words, the significance of the proportionate and non-proportionate step-size distribution with respect to each filter coefficient varies with  $\alpha_{\text{IP}}$ . To allow IPNLMS to converge faster than NLMS and PNLMS regardless of the impulse response nature, it was shown in [8] that good choices of  $\alpha_{\text{IP}}$  values are 0,  $-0.5$  and  $-0.75$ . In contrast to such *fixed* weighting factor, our objective in this paper is to propose a variable weighting factor  $\alpha(n)$  that correlates with the sparseness variation of the adaptive filter so as to improve the tracking capability of echo path changes for the resultant adaptive algorithm.

### 2.2 The MDF and IPMDF algorithms

The MDF algorithm [10] was proposed to mitigate the problem of delay inherent in FLMS [9] since the latter computes the output only every  $L$  samples. In the MDF structure, the adaptive filter of length  $L$  is partitioned into  $K$  subfilters each of length  $N$  with  $L = KN$ . Consequently, the delay of MDF is reduced by a factor of  $L/N$  compared to FLMS.

To describe the MDF algorithm, we first define  $m$  as the frame index and the following time-domain quantities given by  $\mathbf{X}(m) = [\mathbf{x}(mN) \dots \mathbf{x}(mN + N - 1)]$ ,  $\mathbf{y}(m) = [y(mN) \dots y(mN + N - 1)]^T$ ,  $\hat{\mathbf{h}}(m) = [\hat{\mathbf{h}}_0^T(m) \dots \hat{\mathbf{h}}_{K-1}^T(m)]^T$ ,  $\hat{\mathbf{y}}(m) = [\hat{y}(mN) \dots \hat{y}(mN + N - 1)]^T = \mathbf{X}^T(m)\hat{\mathbf{h}}(m)$ ,  $\mathbf{e}(m) = \mathbf{y}(m) - \hat{\mathbf{y}}(m)$ , where  $\hat{\mathbf{h}}_k(m) = [\hat{h}_{kN}(m) \dots \hat{h}_{kN+N-1}(m)]^T$  is the  $k$ th subfilter for  $k = 0, \dots, K-1$ . The  $2N \times 1$  input vector

$$\chi(m-k) = [x(mN - kN - N) \dots x(mN - kN + N - 1)]^T \quad (6)$$

hence denotes the  $k$ th input block. Define next  $\mathbf{F}$  as the Fourier matrix, the  $2N \times 2N$  diagonal matrix

$$\mathbf{D}(m-k) = \text{diag}\{\mathbf{F}\chi(m-k)\} = \text{diag}\{\underline{\chi}(m-k)\} \quad (7)$$

is obtained with elements containing the Fourier transform of  $\chi(m-k)$ . With the following frequency-domain quantities  $\underline{\mathbf{y}}(m) = \mathbf{F} \begin{bmatrix} \mathbf{0}_{N \times 1} \\ \mathbf{y}(m) \end{bmatrix}$ ,  $\underline{\hat{\mathbf{h}}}_k(m) = \mathbf{F} \begin{bmatrix} \hat{\mathbf{h}}_k(m) \\ \mathbf{0}_{N \times 1} \end{bmatrix}$ ,  $\underline{\mathbf{e}}(m) = \mathbf{F} \begin{bmatrix} \mathbf{0}_{N \times 1} \\ \mathbf{e}(m) \end{bmatrix}$ ,  $\mathbf{G}^{01} = \mathbf{F}\mathbf{W}^{01}\mathbf{F}^{-1}$ ,  $\mathbf{W}^{01} = \begin{bmatrix} \mathbf{0}_{N \times N} & \mathbf{0}_{N \times N} \\ \mathbf{0}_{N \times N} & \mathbf{I}_{N \times N} \end{bmatrix}$ ,  $\mathbf{G}^{10} = \mathbf{F}\mathbf{W}^{10}\mathbf{F}^{-1}$  and  $\mathbf{W}^{10} = \begin{bmatrix} \mathbf{I}_{N \times N} & \mathbf{0}_{N \times N} \\ \mathbf{0}_{N \times N} & \mathbf{0}_{N \times N} \end{bmatrix}$  where  $\mathbf{0}_{N \times N}$  is an  $N \times N$  null matrix and  $\mathbf{I}_{N \times N}$  is an  $N \times N$  identity matrix, the MDF algorithm can be described by [10]

$$\underline{\mathbf{e}}(m) = \underline{\mathbf{y}}(m) - \mathbf{G}^{01} \sum_{k=0}^{K-1} \mathbf{D}(m-k) \underline{\hat{\mathbf{h}}}_k(m-1), \quad (8)$$

$$\mathbf{S}_{\text{MDF}}(m) = \lambda \mathbf{S}_{\text{MDF}}(m-1) + (1 - \lambda) \mathbf{D}^*(m) \mathbf{D}(m), \quad (9)$$

$$\hat{\underline{\mathbf{h}}}_k(m) = \hat{\underline{\mathbf{h}}}_k(m-1) + \mu \mathbf{G}^{10} \mathbf{D}^*(m-k) \times [\mathbf{S}_{\text{MDF}}(m) + \delta_{\text{MDF}}]^{-1} \underline{\mathbf{e}}(m), \quad (10)$$

where  $*$  denotes complex conjugate,  $0 \ll \lambda < 1$  is the forgetting factor and  $\mu = \beta(1 - \lambda)$  is the step-size with  $0 < \beta \leq 1$ . Letting  $\sigma_x^2$  be the input signal variance, the initial regular-

ization parameters [1] are  $\mathbf{S}_{\text{MDF}}(0) = \sigma_x^2/100$  and  $\delta_{\text{MDF}} = 20\sigma_x^2 N/L$ . For  $N = L$  and  $K = 1$ , MDF is equivalent to FLMS [9].

The IPMDF algorithm [11] was proposed to combine the fast convergence of IPNLMS and efficient implementation brought about by the MDF structure. To achieve this, the step-size control matrix with diagonal elements given by (5) is imposed to each subfilter  $\hat{\mathbf{h}}_k(m)$  in the time domain such that

$$q_{kN+l}(m) = \frac{1 - \alpha_{\text{IPMDF}}}{2L} + \frac{(1 + \alpha_{\text{IPMDF}})|\hat{h}_{kN+l}(m)|}{2\|\hat{\mathbf{h}}(m)\|_1 + \varepsilon} \quad (11)$$

for  $k = 0, 1, \dots, K-1, l = 0, 1, \dots, N-1$ , and

$$\mathbf{Q}_k(m) = \text{diag}\{q_{kN}(m) q_{kN+1}(m) \dots q_{kN+N-1}(m)\}. \quad (12)$$

Accordingly, the filter coefficients adaptation is performed in the time domain by using (8), (9) and

$$\hat{\mathbf{h}}_k(m) = \hat{\mathbf{h}}_k(m-1) + L\mu \mathbf{Q}_k(m) \tilde{\mathbf{G}}^{10} \mathbf{D}^*(m-k) \times [\mathbf{S}_{\text{IPMDF}}(m) + \delta_{\text{IPMDF}}]^{-1} \mathbf{e}(m), \quad (13)$$

where  $\tilde{\mathbf{G}}^{10} = [\mathbf{I}_{N \times N} \mathbf{0}_{N \times N}] \mathbf{F}^{-1}$ . The initial regularization parameters are given by  $\mathbf{S}_{\text{IPMDF}}(0) = (1 - \alpha_{\text{IPMDF}}) \mathbf{S}_{\text{MDF}}(0)$  and  $\delta_{\text{IPMDF}} = (1 - \alpha_{\text{IPMDF}}) \delta_{\text{MDF}}$ .

### 3. THE SPARSENESS-CONTROLLED IPMDF ALGORITHM

We now incorporate the sparseness control into the IPMDF algorithm. The degree of sparseness for an impulse response can be quantified by [14]

$$\xi(n) = \frac{L}{L - \sqrt{L}} \left( 1 - \frac{\|\mathbf{h}(n)\|_1}{\sqrt{L} \|\mathbf{h}(n)\|_2} \right) \quad (14)$$

for  $0 \leq \xi(n) \leq 1$ , where  $\xi(n)$  is positively correlated with the sparseness and  $\|\cdot\|_2$  denoting the  $l_2$ -norm. In [4], it has been shown that  $\xi(n)$  is inversely proportionate to the distance between the loudspeaker and the microphone. For applications involving hands-free telephony devices, such distance is highly time-varying. Considering such sparseness variation, (14) can be invoked at each iteration allowing an automatic adjustment of the weighting between proportionate and non-proportionate updating of the filter coefficients. The resultant variable weighting factor, as a function of the sparseness of the  $k$ th subfilter

$$\hat{\xi}(m) = \frac{L}{L - \sqrt{L}} \left( 1 - \frac{\|\hat{\mathbf{h}}(m)\|_1}{\sqrt{L} \|\hat{\mathbf{h}}(m)\|_2} \right), \quad (15)$$

gives rise to the proposed SC-IPMDF algorithm.

As mentioned in Section 2, the weighting factor  $\alpha_{\text{IPNLMS}}$  and  $\alpha_{\text{IPMDF}}$  were originally introduced to determine the significance of proportionate and non-proportionate step-size controls. To show the importance of  $\alpha_{\text{IPMDF}}$  for IPMDF in terms of the convergence performance, consider an example case where two AIRs of length  $L = 1024$  were simulated using the method of images [15] in a room of dimension  $8 \times 10 \times 3$  m with 0.57 reflection coefficient and a sampling frequency of 8 kHz. The loudspeaker is fixed at

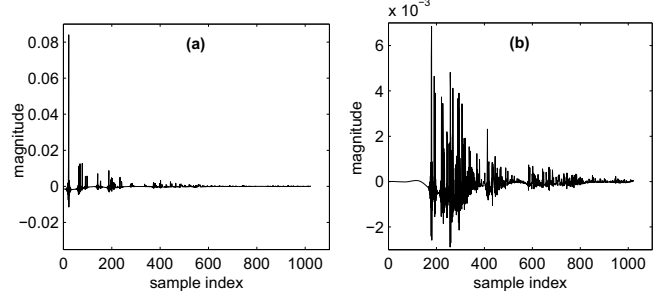


Figure 2: Acoustic impulse responses obtained using the method of images [15] in a room with dimension of  $8 \times 10 \times 3$  m where the distances between the loudspeaker and microphone are (a) 0.9 m and (b) 7.7 m. The resultant sparseness is (a) 0.83 and (b) 0.59 respectively.

$4 \times 9.1 \times 1.6$  m in the LRMS with the distance to the microphone being 0.9 m and 7.7 m so as to obtain AIRs with different sparseness as shown in Fig. 2(a) and Fig. 2(b), respectively. The sparseness measure of these AIRs are computed using (14) giving (a)  $\xi(n) = 0.83$  and (b)  $\xi(n) = 0.59$ . Employing the normalized misalignment given by

$$\eta(n) = \frac{\|\mathbf{h}(n) - \hat{\mathbf{h}}(n)\|_2^2}{\|\mathbf{h}(n)\|_2^2} \quad (16)$$

as the performance measure, the IPMDF algorithm were then tested using a zero mean WGN as inputs while another WGN sequence  $w(n)$  was added to give an SNR of 20 dB. We also assumed that the length of  $\hat{\mathbf{h}}(n)$  is equivalent to that of the unknown  $\mathbf{h}(n)$ .

Figure 3 shows the effect of  $\alpha_{\text{IPMDF}}$  to the performance of IPMDF in terms of  $\eta(n)$  for  $\beta = 0.2, K = 8$  in estimating the AIRs as shown in Fig. 2(a) and Fig. 2(b) respectively. As can be seen, a smaller value of  $\alpha_{\text{IPMDF}}$  is desirable for sparse AIR while  $\alpha_{\text{IPMDF}}$  with larger value is favorable for dispersive AIR. It can be observed that  $\alpha_{\text{IPMDF}} = -0.3$  for sparse identification gives worse initial convergence performance for IPMDF. This is because, when  $\alpha_{\text{IPMDF}} = -0.3$ , it emphasizes more on proportionate term than that for the case when  $\alpha_{\text{IPMDF}} = -0.75$ . Since the  $\|\hat{\mathbf{h}}(m)\|_1$  in (11) is very small during the initial convergence for a sparse impulse response,  $\alpha_{\text{IPMDF}} = -0.3$  results in more noisy step-size and therefore, giving worse initial convergence.

The desired effect can be further verified by plotting  $T_{20}$ , which denotes the minimum time for IPMDF to reach the  $-20$  dB normalized misalignment given a specific  $\alpha_{\text{IPMDF}}$  value, against various sparseness associated with 8 simulated AIRs generated using the aforementioned setup. As it can be seen from Fig. 4 that an approximately monotonic relationship can be observed. By performing a least-squares curve fitting to such relationship, we propose to form a variable weighting factor as a function of  $\hat{\xi}(m)$  such that

$$\alpha_{\text{SC-IPMDF}}(m) = 1 - 2\hat{\xi}(m). \quad (17)$$

As a result, the proposed SC-IPMDF algorithm can be described by (8), (9), (11) - (13), (15) and (17).

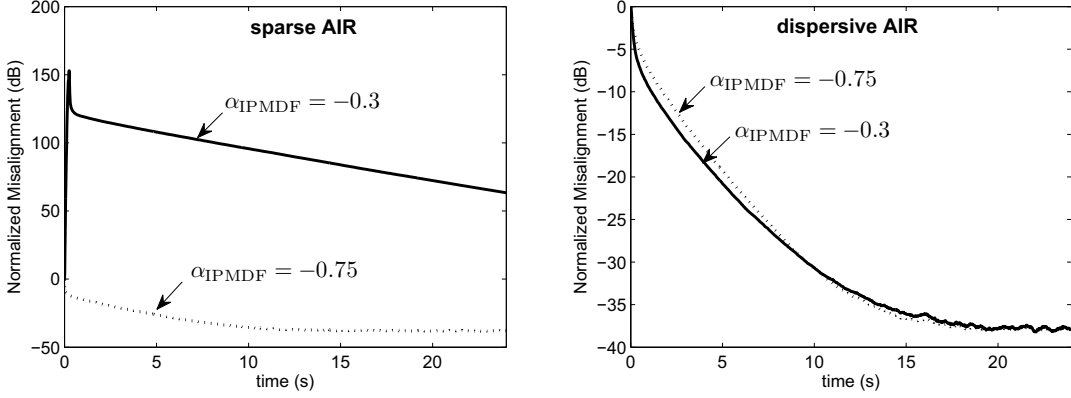


Figure 3: Convergence of IPMDF for different values of  $\alpha_{\text{IPMDF}}$  using WGN input signal. Impulse responses in Fig. 2 (a) and (b) are used as sparse and dispersive AIRs respectively. [ $\beta = 0.2$ ,  $K = 8$ , SNR = 20 dB]

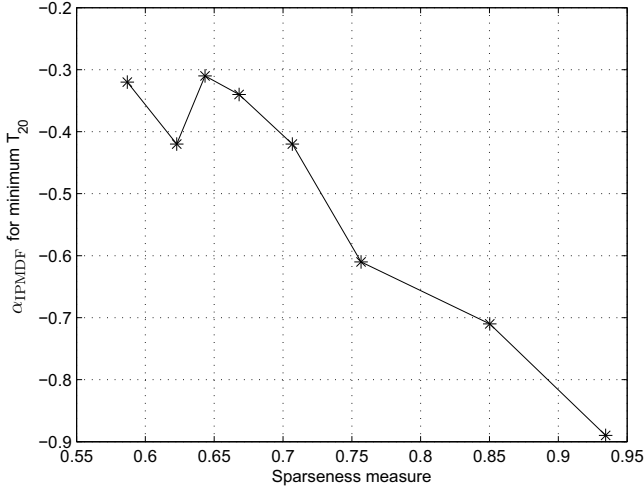


Figure 4: Variation of  $\alpha_{\text{IPMDF}}$  for minimum  $T_{20}$  against AIRs with different sparseness.

#### 4. COMPLEXITY

The relative complexity of MDF, IPMDF and SC-IPMDF in terms of the total number of additions, multiplications and divisions per iteration for adaptation of filter coefficients is shown in Table 1 for  $K = 1$ . Since the IPMDF and SC-IPMDF algorithms update the filter coefficients in time domain, they require additional  $L \log_2(L)$  real multiplications and  $L \log_2(L)$  additions to compute the radix-2 FFT. The additional complexity of the proposed SC-IPMDF also arises from the computation of the sparseness measure  $\hat{\xi}(m)$ . Given that  $L/(L - \sqrt{L})$  in (14) can be computed off-line and that  $l_1$ -norm is available from IPMDF weight updation, the proposed SC-IPMDF only requires additional  $L + 2$  additions,  $L + 3$  multiplications and 1 division, compared to that of IPMDF.

#### 5. SIMULATIONS

We present simulation results to evaluate the performance of the proposed SC-IPMDF algorithm in the context of AEC. A time-varying AIR was obtained by concatenating two simu-

Table 1: Computational complexity of MDF, IPMDF and SC-IPMDF.

| Algorithm | Addition                | Multiplication          | Division |
|-----------|-------------------------|-------------------------|----------|
| MDF       | $4L \log_2(L) + 4L$     | $4L \log_2(L) + 6L$     | $L$      |
| IPMDF     | $5L \log_2(L) + 6L + 2$ | $5L \log_2(L) + 8L + 2$ | $L + 2$  |
| SC-IPMDF  | $5L \log_2(L) + 7L + 4$ | $5L \log_2(L) + 9L + 5$ | $L + 3$  |

lated AIRs as shown in Fig. 2 with two echo path changes being introduced, i.e., from Fig. 2(b) to 2(a) and then back to Fig. 2(b). The convergence performance was measured using  $\eta(n)$  defined in (16). We assumed that the length of  $\hat{\mathbf{h}}(n)$  is equivalent to that of the unknown  $\mathbf{h}(n)$ . Proportionality control factor  $\alpha_{\text{IPMDF}} = -0.75$  was used for the standard IPMDF algorithm and the other simulation parameters were same as in the case described in Section 3.

Figure 5 first compares the convergence performance of MDF, IPMDF and SC-IPMDF using WGN as the input signal. The step-size parameter for each algorithm is set  $\beta_{\text{MDF}} = \beta_{\text{IPMDF}} = \beta_{\text{SC-IPMDF}} = 0.2$ . It can be seen from Fig. 5 that the convergence rate of SC-IPMDF is as fast as IPMDF for dispersive and achieves a faster convergence performance over MDF by up to 7 dB in terms of normalized misalignment. After the echo path change, the SC-IPMDF exhibits a faster tracking performance over both MDF and IPMDF giving approximately 11 dB and 5 dB gain in normalized misalignment, respectively. After the final echo path change, SC-IPMDF maintains its high initial convergence rate over MDF and IPMDF giving respectively 9 dB and 2 dB improvements.

Figure 6 shows the results using a male speech input signal. As can be seen, the proposed SC-IPMDF algorithm achieves the highest rate of convergence, giving approximately 1 dB and 4 dB improvements during initial convergence compared to IPMDF and MDF for the dispersive AIR. For sparse AIR, improvements of up to 3 dB and 7 dB normalized misalignment for SC-IPMDF can be seen in comparison with IPMDF and MDF, respectively. It is also noted that SC-IPMDF achieves better steady-state performance than IP-

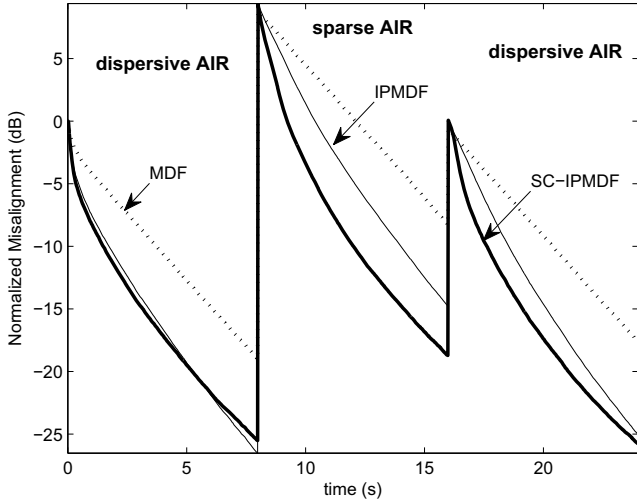


Figure 5: Relative convergence of MDF, IPMDF and SC-IPMDF using WGN input signal with an echo path changes at 8 s and 16 s with  $\beta_{\text{MDF}} = \beta_{\text{IPMDF}} = \beta_{\text{SC-IPMDF}} = 0.2$ ,  $K = 8$ , SNR = 20 dB. The dispersive and sparse AIRs are as shown in Fig. 2(b) and Fig. 2(a) respectively.

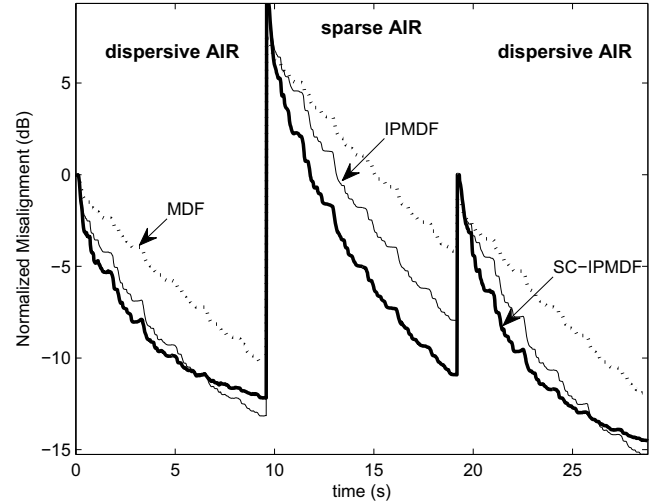


Figure 6: Relative convergence of MDF, IPMDF and SC-IPMDF using speech input signal with an echo path changes at 9.5 s and 19 s with  $\beta_{\text{MDF}} = \beta_{\text{IPMDF}} = \beta_{\text{SC-IPMDF}} = 0.2$ ,  $K = 8$ , SNR = 20 dB. The dispersive and sparse AIRs are as shown in Fig. 2(b) and Fig. 2(a) respectively.

MDF and MDF after the final echo path change.

## 6. CONCLUSIONS

We have proposed SC-IPMDF algorithm for AEC, which integrates the sparseness control mechanism into the MDF structure. This is achieved by forming a variable weighting factor for combining proportionate and non-proportionate tap updating schemes according to the sparseness of the adaptive filter, which allows the proposed SC-IPMDF algorithm to be robust to the sparseness variation of AIRs due to its time-varying nature. The incorporation of the MDF structure ensures a reduced delay for the filter output. Simulation results show an improved convergence and tracking performance in terms of normalized misalignment over MDF and IPMDF algorithms.

## REFERENCES

- [1] J. Benesty, T. Gänslér, D. R. Morgan, M. M. Sondhi, and S. L. Gay, *Advances in Network and Acoustic Echo Cancellation*. Springer, 2001.
- [2] S. Haykin, *Adaptive Filter Theory*, 4th ed. Upper Saddle River, N.J.: PTR Prentice-Hall Inc., 2002.
- [3] Y. Huang, J. Benesty, and J. Chen, *Acoustic MIMO Signal Processing*. Berlin, Germany: Springer, 2006.
- [4] P. Loganathan, A. W. H. Khong, and P. A. Naylor, "A sparseness controlled proportionate algorithm for acoustic echo cancellation," in *Proc. European Signal Processing Conf. (EUSIPCO)*, Lausanne, Switzerland, Aug. 2008.
- [5] D. L. Duttweiler, "Proportionate normalized least mean square adaptation in echo cancellers," *IEEE Trans. Speech Audio Processing*, vol. 8, no. 5, pp. 508–518, Sep. 2000.
- [6] J. Radecki, Z. Zilic, and K. Radecka, "Echo cancellation in IP networks," in *Proc. Forty-Fifth Midwest Symposium on Circuits and Systems*, vol. 2, Tulsa, USA, Aug. 2002, pp. 219–222.
- [7] A. Deshpande and S. L. Grant, "A new multi-algorithm approach to sparse system adaptation," in *Proc. European Signal Processing Conf. (EUSIPCO)*, Antalya, Turkey, Sept. 2005.
- [8] J. Benesty and S. L. Gay, "An improved PNLMS algorithm," in *Proc. IEEE Int. Conf. Acoust., Speech, Signal Processing (ICASSP)*, vol. 2, Orlando, USA, May 2002, pp. 1881–1884.
- [9] E. R. Ferrara, "Fast implementations of LMS adaptive filters," *IEEE Trans. Acoust., Speech, Signal Processing*, vol. 28, pp. 474–475, 1980.
- [10] J. S. Soo and K. K. Pang, "Multidelay block frequency domain adaptive filter," *IEEE Trans. Acoust., Speech, Signal Processing*, vol. 38, no. 2, pp. 373–376, Feb. 1990.
- [11] A. W. H. Khong, P. A. Naylor, and J. Benesty, "A low delay and fast converging improved proportionate algorithm for sparse system identification," *EURASIP Journal on Audio, Speech, and Music Processing*, vol. 2007, Article ID 84376, 8 pages, Jan. 2007.
- [12] R. Ahmad, A. W. H. Khong, and P. Naylor, "Proportionate frequency domain adaptive algorithms for blind channel identification," in *Proc. IEEE Int. Conf. Acoust., Speech, Signal Processing (ICASSP)*, Toulouse, France, May 2006.
- [13] A. W. H. Khong and P. A. Naylor, "Efficient use of sparse adaptive filters," in *Proc. Fortieth Asilomar Conference on Signals, Systems and Computers*, Pacific Grove, California, USA, Oct. 2006, pp. 1375–1379.
- [14] J. Benesty, Y. A. Huang, J. Chen, and P. A. Naylor, "Adaptive algorithms for the identification of sparse impulse responses," in *Selected methods for acoustic echo and noise control*, E. Hänsler and G. Schmidt, Eds. Springer, 2006, ch. 5, pp. 125–153.
- [15] J. B. Allen and D. A. Berkley, "Image method for efficiently simulating small room acoustics," *J. Acoust. Soc. Am.*, vol. 65, no. 4, pp. 943–950, April 1979.